

TIME-DEPENDENT SIMULATIONS OF SOLAR WIND INCLUDING THE TRANSITION REGION

R. Grappin¹, J. Léorat¹ and Y.-M. Wang²

Abstract. A low resolution 1D numerical model of the solar wind including the transition region and a part of the low, cold solar atmosphere is proposed. It is meant as a first step toward multidimensional modeling of wave transfer through the transition region and subsequent heating and acceleration of the corona and wind.

1 Introduction

Solar wind simulations have often been made starting from the middle of the transition region or above (see e.g. Lionello et al. 2001, Endeve et al. 2003). However, when dealing with problems which involve the detailed transfer of waves through the solar atmosphere, which is important when one is interested in the issue of acceleration and heating by such waves, it is important to include also, in a way or another, the coolest part of the atmosphere, and some representation at least of the chromospheric transition region. Recently, Suzuki and Inutsuka (2005) showed that it was possible to both generate the transition region, the hot corona, and generate the supersonic solar wind with acceptable properties by using 1-D fluid MHD simulations in which the Alfvén waves drive compressible waves which dissipate in the corona. However, their simulations used 14000 grid points, which seems to be out of reach in multidimensional situations. One of our motivations here is to investigate the possibility of reproducing such results using a much lower number (300) of grid points. The second motivation is to have a simple tool at hand to explore the effect of varying physical parameters such as the magnetic expansion factor. As a first step, we report here simulations in a purely hydrodynamic framework, in which the heat input is modeled using a standard expression, instead of direct viscous or ohmic dissipation.

2 The stationary regime

Before describing the details of the model and method, let us first give a brief account of the properties of the solution obtained in the quasi-steady state regime, reached after a large number of time steps. Figure 1 shows the density and the temperature. A transition region is seen to occur at about $0.015 R_s = 10\,000$ km. The temperature has a minimum about 6000 K at the bottom, and a maximum around 1.6 MK, around 4 solar radii. The sonic Mach number (Fig. 2) is reached at about 5 solar radii. In the simulated domain, from 1 up to 15 solar radii, the density drops by a factor 10^{-16} .

3 Equations, model and method

The equations are the one-dimensional gas equations with spherical symmetry. We use a non-uniform mesh with 300 points following a logarithmic progression of ratio $q=1.025$. This corresponds to a minimum mesh size being $\Delta r = 10^{-4}R_s = 70$ km at the surface, and a maximum mesh $\Delta r = 0.4R_s$ at the outer boundary ($r = 15R_s$). Our temporal scheme is Runge-Kutta of order 3; the spatial scheme is a compact finite difference scheme of order 6 (Lele 1993). Note however that to compute the temperature gradients which appear in the conductive term, we use a scheme of order two.

¹ Observatoire de Paris, LUTH, CNRS UMR 8102, 92195 Meudon, France

² Code 7672W, E.O. Hulburt Center for Space Research, Naval Research Laboratory, Washington DC 20375-5352, USA

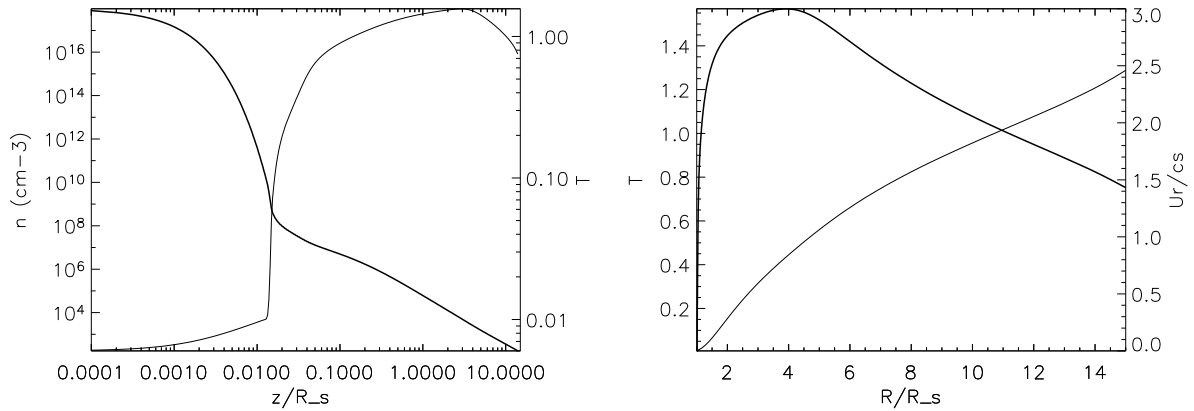


Fig. 1. Main profiles at time $t = 40$. Left: density and temperature versus altitude z ; right: temperature and Mach number versus heliocentric distance R .

We describe here the energy equation, which reads in terms of the pressure P :

$$\partial P/\partial t + u\partial P/\partial r + \gamma P \text{div} u = (\gamma - 1)(Q_h - n^2\Lambda(T) - \text{div} q_c) \quad (3.1)$$

where Q_h is the coronal heating source, Λ the radiative loss function (Rosner et al. 1978), and $q_c = -\kappa\hat{e}_r\partial T/\partial r$ the heat flux. The heating function has the exponential form: $Q_h = A(1/r^2)\exp(-(r-1))$ where A is such that the heat flux at the solar surface is $10^5 \text{ erg/cm}^2/\text{s}$.

The conductive heat flux q_c is defined in several steps. We start with the Spitzer-Harm expression $q_{SH} = \kappa_0 T^{5/2} \partial T/\partial x$ where $\kappa_0 = 10^{-6} \text{ erg/cm/s/K}^{7/2}$. This form being highly demanding in computer resources (and mesh size), we consider a “smoothed Spitzer-Harm” heat flux q_{SSH} equal to the previous expression for temperatures higher than 1MK, but with a smoother (linear) temperature dependence for conductivity at low temperature. This is similar to the prescription first proposed by Linker et al. (2001). Last, we take partly into account the fact that the resulting flux exceeds soon the ballistic flux $q_{bal} = 3/2 P c_s$ (c_s being the sound speed): we thus multiply the smooth SH flux by a ramp function centered around $2R_s$ with width $1R_s$. The resulting ramp thus goes from 0.9 to 0.01 from $R=1$ to $R=15$ solar radii.

The various steps of the construction of the conductive flux are shown in Fig.2, left panel, in arbitrary units. The conductive flux is computed from the temperature profile at time $t=40$. The Spitzer-Harm expression (SH) appears with dashes; the smoothed SH is drawn as a plain line; the ballistic “flux” (with a -1 factor to help comparison) is drawn with dots. The final smoothed SH flux multiplied by the ramp appears as a thick line.

One sees that the smoothed SH flux is largely different from the original SH flux at low temperatures, as expected. Note that the ballistic flux is exceeded by the collisional expressions (SH or smoothed SH) as soon as at $R = 1.1R_s$. This lasts up to about 3 solar radii. This situation is only slightly cured by the ramp function.

The three source terms for the temperature equations (that is, the source terms in equation (3.1) for the pressure, but divided by the density), are shown in Fig.3, right panel, in arbitrary units. The temperature is also shown for reference. One sees that the conductive and radiative loss terms compensate around the transition region while, above, the coronal heating term balances the conductive term, with a peak around $R=2$ solar radii, as expected by the definition.

The calculation which produced the results shown above starts at time $t=0$ from a static atmosphere at hydrostatic equilibrium, which is cold (6000 K) everywhere. Because of this, the scale height is small, and the density very low. The method used to go from this initial state to the final wind with hot corona, after a time lapse of $\Delta t = 40$, that is 30 hours, is made of several steps. Indeed, the density being extremely low at the initial state, we cannot reasonably hope to immediately integrate the equations described above with a limited number of grid points (300 here), even with a very non-uniform mesh. Hence we consider a first short period (lasting from $t=0$ up to $t=1$) during which we pass from the initial very cold atmosphere to a much warmer state, using a modified setup. During this first period, we integrate only the equation for the temperature, and

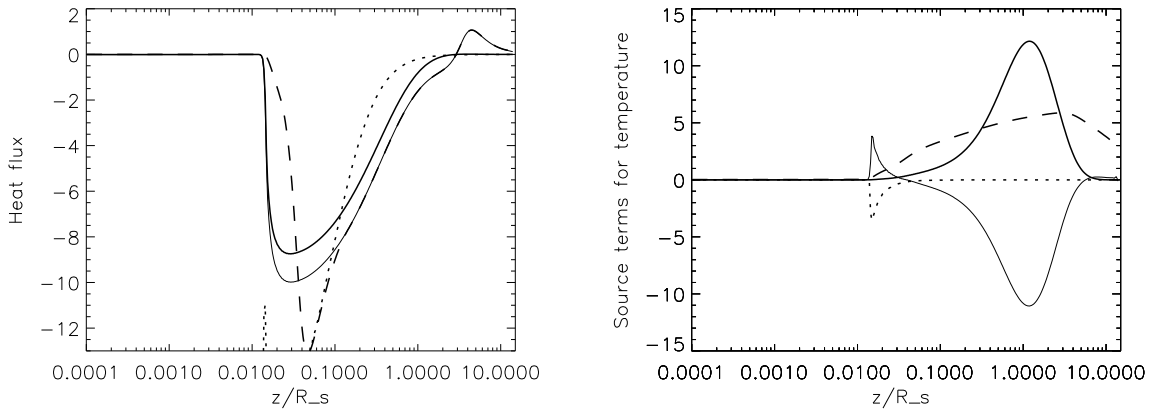


Fig. 2. Heat sources (arbitrary units) versus altitude. Left: Several forms of the conductive heat flux associated with the temperature profile at time $t = 40$. Spitzer flux; smooth Spitzer flux; ballistic flux (multiplied by -1); smooth Spitzer flux multiplied by a ramp function (actual heat flux). Right: The three source terms for temperature: Coronal heating term (thick); radiative term (dotted); conductive term (plain). Temperature (dashed) is represented for reference.

deduce the pressure by solving the hydrostatic equilibrium equation. The velocity thus remains zero up to time $t=1$. After that period, we relax this condition, and the quasi-hydrostatic equilibrium which has been reached at time $t=1$ serves as an initial condition for the computation. The hydrostatic phase is actually divided in two parts: during the first half (from $t=0$ to 0.5), the temperature source terms are simplified, and are considered fully only when $t > 0.5$. Specifically, during the phase from $t=0$ up to $t=0.5$, conductivity varies everywhere linearly with temperature, and, moreover, the whole conductive source term for the temperature is limited by an upper bound (so that the energy equation is not conservative). This preliminary unphysical phase has proved necessary, in order to reach a quasi-static equilibrium in a reasonable time.

The boundary conditions are imposed via the characteristic form of the equations. They are: no incoming perturbation at the inner boundary, and, starting with time $t=1$, a constant depression at the outer boundary, introduced via the ingoing characteristics. This suction stops as soon as the sonic Mach number is reached, since thereafter no incoming signal can progress into the domain from the exterior.

4 Temporal evolution

We have described with some details the quasi-stationary state obtained after a long time, about $t=40$, about 30 hours (unit time being 1h30). As just described, the full equations are integrated starting from time $t=1$, with at that time a state which is quasi-static, but already has large temperature gradients. Two factors contribute to generate the supersonic wind regime at $t=1$. The main one is that the thermal profile has no reason to be at equilibrium (the temperature equation is changed at that time). Second, we introduce a suction at the external boundary, using the ingoing characteristics, in order to trigger an outward flow, as mentioned above. In fact, this latter effect appears secondary: it essentially limits the occurrence of accretion at the outlet during the early phase.

The resulting evolution is shown in Fig.3. The left panel shows the temperature from $t=1$ up to $t=40$, every $\Delta t = 1$, and the right panel shows the Mach number. The temperature of the corona is seen to stabilize very soon, at time $t=3$ in most of the domain, except for the very outer part from $R=12$ up $R=15 R_s$, where the relaxation takes a longer time. Although it essentially stops after time $t=3$, the early temperature oscillation is the direct cause of the huge velocity perturbation which progresses, and grows, through the corona and finally sets up the supersonic wind.

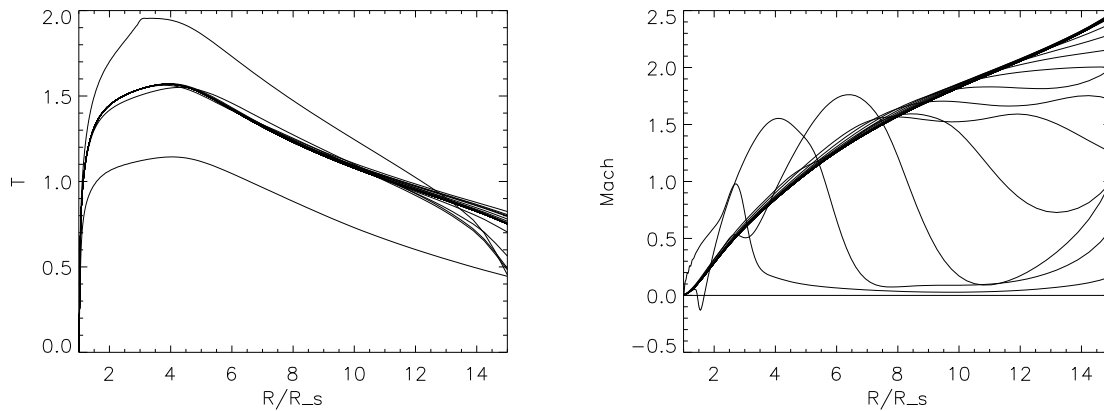


Fig. 3. Successive profiles of temperature (left) and Mach number (right), at times $t=1, 2, \dots, 40$.

5 Discussion

Our numerical 1D model allows to obtain, with a limited number of grid points (300), a strongly stratified atmosphere (including a model of the transition region) and a supersonic wind. The domain goes from the surface up to $15R_s$. The wind becomes stationary in a short time. For instance, stationarity is obtained up to $R = 8R_s$ after a time $t=5$ (see Fig.3), that is, about 100 000 time steps.

An important trick to arrive at this result was to set up a preliminary unphysical preparation phase (up to $t=1$) during which the atmosphere is heated hydrostatically, which then provides a starting point for a true dynamical integration. Note that this preparation phase seems to be unnecessary in Suzuki and Inutsuka's (2005) work, probably because of the very large resolution they use.

An issue of physical importance is that of the modelization of the conductive heat flux in the non-collisional regime. We have had no difficulty in adding a free streaming contribution of the form $(3/2Pu)(1 - H(r))$, that is, using the same ramp function $H(r)$ centered on $r = 2R_s$ as the one used to "mild" the collisional heat flux (see above). The (expected) result was that the effective adiabatic index passes from $\gamma = 5/3$ to $\gamma_{eff} = 4/3$, this being visible in the distant decrease rate of temperature (Hollweg 1976). However, the question is not solved so simply at closer distances. Indeed, we have seen (Fig.2) that in our model the conductive heat flux exceeds the ballistic evaluation already very largely at $R = 2R_s$. Our preliminary attempts to decrease the conductive flux expression in the region below have up to now led to unphysically large time-dependent deviations of temperature and speed. We plan to progress in this direction, taking into account in particular the study by Holzer and Leer (1981).

Our second objective will be to replace the ad hoc heating term by the viscous and ohmic dissipation terms, in the MHD framework. Also, we plan to study the consequence of the strong stratification due to heating on 2D and 3D wave transfer and coupling with wind (see Grappin, Léorat & Habbal 2005).

References

- Endeve, E., Leer, E., Holzer, T. 2003, ApJ, 589, 1040
- Grappin, R., Léorat, J., Habbal, S. R. 2005 A&A, 437, 1081
- Hollweg, J.V. 1976, J. Geophys. Res., 81, 1649
- Holzer, T.E., Leer, E. 1981, J. Geophys. Res., 85, 4665
- Lele S.K. 1992, J. Comput. Phys. 103, 16
- Linker, J.A., Lionello, R., and Mikic, Z. 2001, J. Geophys. Res. 106, 25165
- Lionello, R., Linker, J.A., and Mikic, Z. 2001, ApJ, 546, 542
- Rosner, R., Tucker, W. H., and Vaiana, G. S. 1978, ApJ, 220, 643
- Suzuki, T.-K. and Inutsuka, S. 2005, ApJ., 632, L49